Journal of the Korean Ceramic Society
Vol. 44, No. 7, pp. 354~357, 2007.

The Effect of the Sintering Additives on the Fabrication and Thermal Conductivity of Porous Sintered RBSN

Young-Jo Park† and Hai-Doo Kim

Powder Materials Research Division, Korea Institute of Materials Science, Changwon, 641-010, Korea
(Received June 29, 2007; Accepted July 23, 2007)

ABSTRACT

The nitriding and post-sintering behavior of silicon powder compact containing sintering additives of 2.3 wt% and 7 wt% were investigated in this study. Regardless of the liquid phase content, elongated large grains of a typical morphology evolved in the post-sintered specimens. Phase analysis revealed a complete phase transformation into β-Si_3N_4 in both porous systems. Oxynitride second phases (mellilite) precipitated in the latter, while those were free in the former containing less amount of liquid phase. The post-sintering condition that yielded a favorable microstructure for a filter application was achieved when the specimens were soaked at 1800°C for 2 h. It was found that the thermal conductivity of porous Si_3N_4 ceramics is dominated by the porosity more than this factor is influenced by the addition of Al_2O_3.

Key words*: *RBSN, SRBSN, DPF, Porous, Thermal conductivity

1. Introduction

In addition to providing machinability, porous ceramic materials have many industrial applications as filtering media including high-temperature gas filters, separation membranes, and catalyst supports. Recently in Europe, the market share of diesel vehicles among newly built passenger cars exceeded 50 percents and this rate continues to increase. A diesel particulate filter (DPF) is a component that traps and eliminates particulate matter (PM) contained in the exhaust gas of diesel-powered vehicles.[1] In advanced countries, the attachment of DPFs onto diesel vehicles is required by law. Nevertheless, only limited efforts have been made to replace the currently commercialized cordierite and/or SiC filter in DPFs with Si_3N_4 ceramics.[2]

The addition of sintering aids is indispensable for the densification of Si_3N_4 ceramics fabricated by both gas pressure sintering and pressureless sintering. The composition and quantity of sintering aids decisively controls the extent of grain growth, grain morphology and the precipitation of second phases.[3] The authors, however, could not identify previous reports dealing with the aforementioned phenomena investigated in porous Si_3N_4 ceramics.

In this study, metal silicon powder, which is much cheaper than Si_3N_4 powder, was selected as a starting material, and a reaction-bonding process[4,5] followed by post-sintering[6,7] was employed to produce a porous Si_3N_4 filter substrate. Based on the typical intermingled columnar microstructure of Si_3N_4 ceramics, the goal of this research is to develop a filter substrate exerting the maximum permeability and soot trap performance simultaneously. Emphasis was placed on the relationship between the additive content and the microstructure, as well as on the effect of the additive composition on the thermal conductivity of porous reaction-bonded silicon nitride (RBSN) and sintered-RBSN (SRBSN).

†Corresponding author : Young-Jo Park
E-mail : yjpark87@kims.re.kr
Tel : +82-55-280-3356 Fax : +82-55-280-3392

2. Experimental Procedure

The raw Si materials used in this study were commercially available. Commonly used sintering additives for the sintering of Si_3N_4 ceramics, Y_2O_3 (H.C. Starck, Grade C) and Al_2O_3 (Sumitomo, AKP-30), were selected. Powder mixtures were made either by a single addition of rare earth oxide (designated as Y) or a concurrent addition of Y_2O_3 and Al_2O_3 (designated as YA). The total amount of sintering additives was fixed at 2.3 wt% and 7 wt%, respectively, for the two aforementioned cases. A spherical-shaped pore former (PMMA, Aldrich) was blended in order to control the porosity level of the sintered body. Various combinations of the sintering additive and pore former are listed in Table 1 along with their nomenclature.

Approximately 50 g of powder mixture consisting of Si, sintering additives and pore former were thoroughly milled in a nylon jar with Si_3N_4 balls and ethanol as milling media for 7 h. After the powder mixtures were dried using a rotating evaporator, they were sieved to a particle size < 150 μm.

Table 1. Composition of the Si Powder Mixture

(Unit : g)

	Si	Y_2O_3	Al_2O_3	PMMA
2.3YAP0	100	3.12	0.88	-
2.3YP0	100	4	-	-
2.3YAP20	100	3.12	0.88	20
2.3YP20	100	4	-	20
7YAP20	100	9.66	2.73	20

The resulting powder mixtures were uniaxially pressed into rectangular pellets measuring 10 mm×10 mm ×1.3 mm and were subsequently cold isostatically pressed at 200 MPa. After shaping, the samples were heated in a 95% N_2+5% H_2 flowing atmosphere at temperatures ranging from 1250°C to 1350°C using a horizontal tube furnace in which reaction-bonding occurred. A maximum of eight specimens were placed upon a suspended BN-coated graphite plate. The specimens were erected upright on their edges and made to fit into a small hole on a graphite plate so that both the chance for contamination and the temperature gradient in the specimen were minimized with minimum contact between the specimens and the graphite plate. The percent of nitridation was calculated from the weight change before and after the nitriding process. In preparation for the post-sintering of the nitrided specimens, samples taken from the nitriding furnace were placed upon a BN-coated graphite crucible with Si_3N_4 powder filling the volume of the crucible. Post-sintering was carried out in a graphite resistance furnace both at 1700°C and 1800°C under a static nitrogen gas pressure of 0.9 MPa. SEM (Jeol, JSM-6700F, Japan) was used to observe the fracture surfaces, and X-ray diffraction (Rigaku, D/Max 2200, Japan) was performed for the phase identification. The thermal conductivity (K) at room temperature was calculated from the measured thermal diffusivity (α) using a micro-flash machine (MicroFlash, LFA437, Germany) together with the measured density (ρ) and known heat capacity (c_p), $K\ (W/mK)=\rho \cdot c_p \cdot \alpha$.

3. Results and Discussion

A volume increase of 21.4% and weight gain of 66.5% occurred by the nitriding reaction of $3Si(s)+2N_2(g)$ $Si_3N_4(s)$. Assuming perfect nitridation of raw Si powder and zero loss during the entire process, the theoretical porosity of RBSN and SRBSN can be calculated.[8] In Fig. 1, the measured porosity values (scattered dots) are plotted together with the calculated values (solid lines) for 20 parts of pore former content with a fixed sintering additive of 2.3 wt%. More than 45% porosity was readily achieved by post-sintering up to 1700°C, at which temperature shrinkage was restricted within 1%~2%. A constant tendency was found in which the measured values are somewhat larger than the calculated values. This discrepancy can be attributed to the weight loss caused by evaporation during the process.

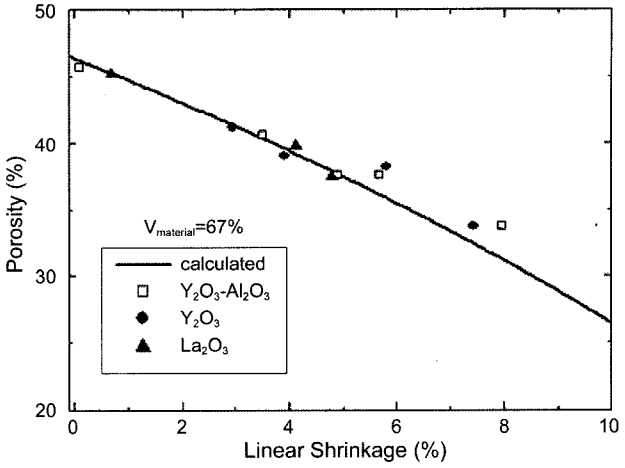

Fig. 1. Measurement (scattered dots) and calculation (solid line) of the porosity for specimens blended with 20 parts of pore former: The amount of sintering additive was fixed at 2.3 wt%.

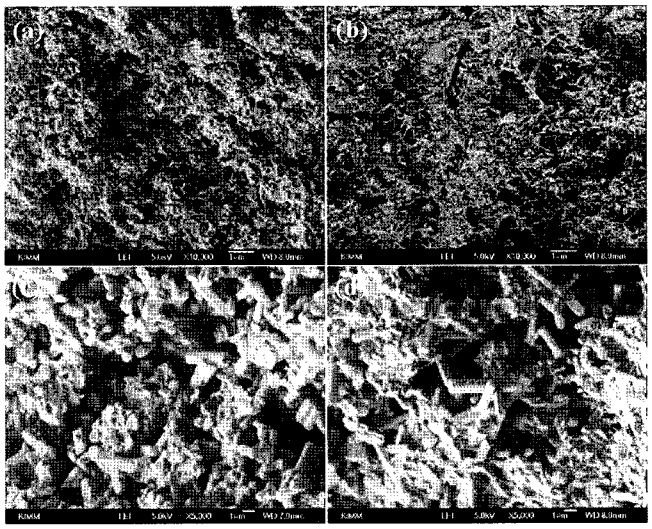

Fig. 2. Fracture surface of RBSN (a,b) and SRBSN (c,d): Insets (a,c) and (b,d) are for 2.3YAP20 and 7YAP20, respectively. Reaction bonding of Si compact was conducted at 1350°C and subsequent post-sintering was conducted at 1800°C for 2 h in a 0.5 MPa nitrogen atmosphere.

The microstructures of the RBSN specimens (Figs. 2(a) and (b)) consist of equiaxed matrix grains and whisker-like grains with diameters of a few hundred nanometers. The starting raw Si powder (d_{50}=7 μm) were shattered into smaller Si_3N_4 particles by the nitriding reaction. It is interesting to note the very similar same grain morphology and pore structure of SRBSN between the 2.3 wt% system and 7 wt% system. The fracture surfaces of both specimens post-sintered at 1800°C show a well-developed three-dimensional array of elongated grains. In addition, the coalescence of pores proceeded during the post-sintering stage together with the grain growth. Much of the commercial products of dense Si_3N_4 ceramics fall in the composition range similar to

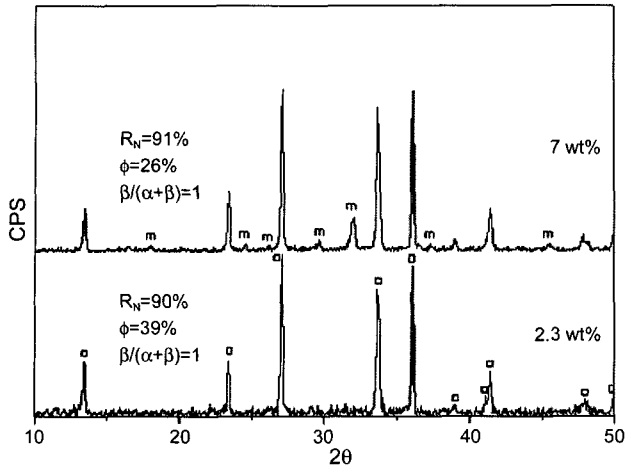

Fig. 3. Phase analysis of a post-sintered specimen: Complete phase transformation into β-Si_3N_4 was confirmed for both 2.3YAP20 and 7YAP20. The lower additive system (2.3 wt%) was verified to be second-phase-free.

5 wt%Y_2O_3-2 wt%Al_2O_3, i.e., a 7 wt% additive system. Obtaining a similar microstructure with less sintering additive, 2.3 wt% in this research, bears some engineering importance considering that this is associated with less shrinkage due to the lower liquid phase content. A suitable porosity and pore channel structure for a filter application is apt to be acquired in the system in which shrinkage is kept to a minimum level.

A phase analysis conducted for the SRBSN specimens is plotted in Fig. 3, in which R_N, ϕ and β/(α+β) are the nitridation rate, porosity and β-Si_3N_4 phase fraction, respectively. For the RBSN specimens, all of the parameters mentioned above are similar each other independent of the amount of sintering additives. In contrast, a higher porosity was measured in the 2.3 wt% system compared to the 7 wt% system for the post-sintered specimens. It should be noted that the 2.3 wt% specimen was free from oxynitride second phases (designated as m), which are deteriorating to the material properties. By reducing the sintering additive content from 7 wt% to 2.3 wt%, a second-phase-free and higher porosity filter substrate was obtained successfully.

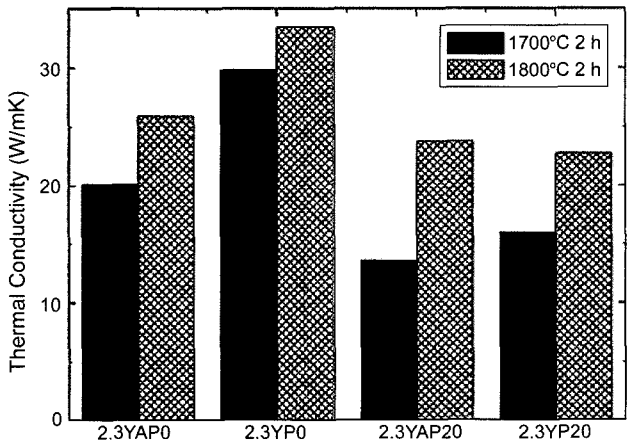

Fig. 4. Thermal conductivity of porous Si_3N_4 ceramics with 2.3 wt% additive: The addition of Al_2O_3 decreases the thermal conductivity in specimens free from pore former, while a negligible effect was revealed for the porous specimens blended with pore former.

The incorporation of aluminum and oxygen in the Si_3N_4 structure decreases the thermal conductivity because substituted ions and vacancies for charge neutrality act as a phonon scattering site.[9] The measurement of thermal conductivity was carried out for the 2.3 wt%-additive specimens, which are better suited for a filter application. For specimens free from pore former, the thermal conductivity of the 2.3YP0 specimen is higher than that of 2.3YAP0 specimen, which was blended with Al_2O_3 as a sintering additive. Only a fractional difference existed in the measured thermal conductivity between Al_2O_3-added (2.3YAP20) and Al_2O_3-free (2.3YP20) samples when pore former was mixed to increase the porosity. It is believed that the larger porosity with the addition of pore former dominated the decrease in the thermal conductivity. The addition of Al_2O_3 has a negligible influence on the thermal conductivity of highly porous Si_3N_4 ceramics.

4. Conclusions

In order to develop microstructure controlling technology of porous RBSN and SRBSN for a DPF application, the effect of additive contents and composition was investigated. An elongated grain microstructure was obtained in as low as a 2.3 wt% additive system. Furthermore, a second-phase-free sound microstructure consisting of only a β-Si_3N_4 phase was fabricated by reducing the additive content. An addition of Al_2O_3 for liquid phase sintering is possible and does not sacrifice the thermal conductivity for in the investigated porous body.

Acknowledgement

This study was supported by the CEFV (Center for Environmentally Friendly Vehicles) of the Eco-STAR project from the MOE (Ministry of the Environment, Republic of Korea).

REFERENCES

1. K. Ohno, K. Shimato, N. Taoka, H. Santae, T. Ninomiya, T. Komori, and O. Salvat, "Characterization of SiC-DPF for a passenger car," *SAE paper No.* 2000-01-0185 (2000).
2. N. Miyakawa, H. Sato, H. Maeno, and H. Takahashi, "Characteristics of Reaction-bonded Porous Silicon Nitride Honeycomb for DPF Substrate," *JSAE Review*, **24** 269-76

(2003).
3. G. Petzow and M. Herrmann, *Silicon Nitride Ceramics; Structure and Bonding*, **102** Springer-Verlag Berlin Heidelberg, 2002.
4. A. J. Moulson, "Reaction-Bonded Silicon Nitride: Its Formation and Properties," *J. Mater. Sci.*, **14** 1017-51 (1979).
5. G. Ziegler, J. Heinrich, and G. Wotting, "Relationships between Processing, Microstructure and Properties of Dense and Reaction-Bonded Silicon Nitride," *J. Mater. Sci.*, **22** 3041-86 (1987).
6. J. A. Mangles and G. J. Tennenhouse, "Densification of Reaction-Bonded Silicon Nitride," *J. Am. Ceram. Soc. Bull.*, **59** 1216-19 (1980).
7. B. T. Lee, J. H. Yoo, and H. D. Kim, "Size Effect of Raw Si Powder on Microstructures and Mechanical Properties of RBSN and GPSed-RBSN Bodies," *Mater. Sci. Eng. A*, **333** 306-13 (2002).
8. Y. J. Park, Eugene Choi, H. W. Lim, and H. D. Kim, "Design of Porosity Level for Porous Si_3N_4 Ceramics Manufactured by Nitriding and Post-Sintering of Si Powder Compact," *Mater. Sci. Forum*, **534-536** 1017-20 (2007).
9. K. Hirao, A. Tsuge, K. Watari, M. Toriyama, and S. Kanzaki, "Thermal Conductivity of β-Si_3N_4: II. Effect of Lattice Oxygen," *J. Am. Ceram. Soc.*, **83** [8] 1985-92 (2000).